STRESS ANALYSIS OF AN HTGR GRAPHITE FUEL ELEMENT INCLUDING RADIATION CREEP AND DIMENSIONAL CHANGES

J. REYNEN, J. BLANCKENBURG, P. DE WINDT, J. PUTZEYS,
Commission of the European Communities
Euratom Joint Nuclear Research Center, Ispra, Italy,

ABSTRACT

A parametric study is presented concerning the stress evolution in an H.T.G.R. graphite fuel element in irradiation environment. Radiation induced creep is taken into account by a linear viscoelastic rheological model, considering elastic behaviour, primary creep and secondary creep. The response to Wigner strains and to thermal dilatation strains is presented.

A numerical example concerning a tubular graphite fuel element is included, making use of a two dimensional finite element code (ROTTEMP).

1. INTRODUCTION

The use of graphite in nuclear reactors dates from the early piles where it has been applied as reflector material. Nowadays graphite is also used in the core of gas cooled reactors as moderator and as structural material. This has led to an increasing effort to characterize the different types of graphite in radiation environment in order to develop a strategy for the designing of core components in graphite. The parameters to be considered for the in-core design are:

- anisotropy
- thermal expansion
- thermal conductivity
- Wigner effect
- Young's modulus and Poisson's ratio
- creep properties in radiation environment
- allowable stresses and rupture criteria

etc.

The design of core components in graphite is the more complex, since its properties are dose and temperature dependent, and they may vary throughout the structure due to unhomogenity. Very often recourse has to be made to simplified models, which do not allow for an exact stress analysis. On the other hand they permit a parametric study, and in the early design stage they facilitate the decisions concerning geometrical lay out and the type of graphite to be chosen.

As to the stress analysis of H.T.G.R. graphite fuel elements, the main sources for stresses are the unhomogeneous thermal dilatation strain field and the unhomogeneous Wigner strain field. Due to irradiation induced creep, stresses generated by these mechanisms tend to relax. At shutdown, however, the relaxed part of the thermal stresses occur with opposite sign.

The calculation of the stress distribution can in principle be carried out by a creep code using empirical creep laws [1], [2], [3]. Due to the many parameters playing a part, the calculations become rather labourious and difficult to interpret.

In this paper a qualitative parametric study is given of the mechanisms defining the stress pattern evolution in H.T.G.R. fuel elements during their life time, including shutdown periods. The irradiation induced creep properties of graphite are represented by a linear visco-elastic rheological model in the dose domain, in conformity with [4] and [5].

A quantitative numerical example is included concerning the stress analysis of a current type of tubular graphite fuel element fot H.T.G.R. .

2. REVIEW OF IN-PILE BEHAVIOUR OF GRAPHITE

2.1 Constitutive Equations

According to [4], [5], [6], [7] the in-pile creep behaviour of a monoaxial graphite specimen can be represented by the visco-elastic rheological model represented in Fig.1 . This model includes elastic behaviour, a recoverable primary creep and a secondary creep (N.B. The dashpots are considered in the dose domain γ rather than in the time domain t).

The response of this system to a stress $\sigma(\gamma)$ is given by the convolution integral: [8]

$$\begin{aligned} \varepsilon(\gamma) &= \int_0^{\gamma} \frac{1}{E} J(\gamma-\gamma') \frac{d\sigma}{d\gamma'} d\gamma' \\ &= \frac{1}{E} J(\gamma) * \frac{d\sigma}{d\gamma} \qquad (1) \\ J(\gamma) &= 1 + a_1 (1 - e^{-\gamma/\gamma_1}) + \gamma/\gamma_2 \end{aligned}$$

γ fast dose

ε strain

σ stress

E Young's modulus

a_1 ratio of fully developed primary creep strain to elastic strain

γ_1 primary creep time constant

γ_2 dose at which secondary creep strain is equal to elastic strain (secondary creep time constant).

2.2 Dimensional Changes

According to [4], [5], [6], [7] the dimensional changes of graphite in radiation environment can be represented by:

$$\varepsilon(\gamma) = b_1 \gamma + b_2 \gamma^2 \qquad (2)$$

The coefficients b_1 and b_2 are functions of temperature, and of the type of graphite.
In Fig.2 are given typical curves for anisotropic Gilsocarbon [8]. Experimental results of other type of graphites show a similar behaviour i.e. a summation of a (negative !) linear ramp function and a (positive) parabolic ramp function.

3. STRESS ANALYSIS WITH VISCO-ELASTIC CONSTITUTIVE EQUATIONS

The stress analysis of a structure of linear visco-elastic material is similar to the elastic analysis under certain assumptions [9]. In order to show this and to discuss the assumptions, the visco elastic stress analysis using the finite element concept, is presented.

The stress distribution in a structure is governed by equilibrium and compatibility interrelated by constitutive relations between stress and strain. An alternative way of analysis consists of minimizing the potential energy of the structure for a virtual displacement field, satisfying the boundary conditions. This principle results in the theorem of virtual work:

$$\iiint \{\delta\varepsilon\}^T\{\sigma\}dV = \iint \{\delta u\}^T\{p\}dF \qquad (3)$$

(notation according to Zienkiewicz [10])

In the linear elastic theory the constitutive equations and the geometrical relations between strain and displacements can be written as:

$$\begin{aligned} \{\sigma\} &= [D](\{\varepsilon\}-\{\varepsilon_0\}) \\ \{\varepsilon\} &= [B]\{u\} \end{aligned} \qquad (4)$$

In the concept of finite elements the integrals of (3) are evaluated piecewicely in terms of a nodal point displacement vector { u }. This results into the relations:

$$\begin{aligned} \{u\} &= [K]^{-1}\{p\} + [K]^{-1}[K_1]\{\varepsilon_0\} \\ \{\sigma\} &= [A_1]\{p\} + [A_2]\{\varepsilon_0\} \end{aligned} \qquad (5)$$

From (5) it is seen that in the elastic analysis displacements, strains and stresses are linearly dependent on load due to external forces and on load due to initial strains.
In view of the application of this solution method, the empirical monoaxial linear viscoelastic constitutive equation (1) is generalized for a three dimensional state of stress:

$$\{\varepsilon\} = [D]^{-1} J * \frac{d\{\sigma\}}{d\gamma} + \{\varepsilon_0\} \qquad (6)$$

The generalization assumes that the Poisson's ratios for the radiation induced creep are equal to the elastic ones. This creep process is therefore assumed to be accompanied with a volume change (more experimental evidence is needed to sustain this assumption).

In order to reduce the algebra it is convenient to introduce Laplace transformations defined by:

$$\begin{aligned} \bar{f}(s) &= \int_0^\infty f(\gamma)\, e^{-s\gamma}\, d\gamma \\ L\, f(\gamma) &= \bar{f}(s) \\ L^{-1}\bar{f}(s) &= f(\gamma) \end{aligned} \qquad (7)$$

The constitutive equation (6) in the Laplace transformed domain becomes:

$$\{\bar{\varepsilon}\} = [D]^{-1}\{\bar{\sigma}\}\bar{J}(s)s + \{\bar{\varepsilon}_0\} \qquad (8)$$

The theorem of virtual work (3) in the Laplace transformed domain becomes:

$$\iiint \{\delta\varepsilon\}^T \{\bar{\sigma}\} dV = \iint \{\delta u\}^T \{\bar{p}\} dF \qquad (9)$$

Introducing (8) into (9), assuming that the creep function $\bar{J}(s)$ is independent of space, yields the relations for displacements and stresses in the Laplace transformed domain:

$$\begin{aligned} \{\bar{u}\} &= [K]^{-1} \{\bar{p}\} \bar{J}(s)s + [K]^{-1}[K_1] \{\bar{\varepsilon}_0\} \\ \{\bar{\sigma}\} &= [A_1]\{\bar{p}\} + [A_2]\{\bar{\varepsilon}_0\}\left[\bar{J}(s)s\right]^{-1} \end{aligned} \qquad (10)$$

Comparison of (5) and (10) shows that under the assumptions of:

(i) generalization of monoaxial in-pile creep data to a three dimensional state of stress and of

(ii) homogeneity of the dose dependent part of the creep function J over the structure, the stress analysis for visco-elastic material is similar to the one for elastic material:

(i) stresses due to external load (primary stresses) are equal to those calculated elastically for the momentary load p(t)

(ii) stresses due to initial strains (secondary stresses) relax homogeneously according to the relaxation function $L^{-1}(\bar{J}(s)s)^{-1}$

(iii) displacements due to external loads creep homogeneously according to the creep function $J(\gamma)$

(iiii) displacements due to initial strains are equal to those calculated elastically for the momentary initial strains $\{\varepsilon_0(\gamma)\}$

A parametric study of the stress evolution during the lifetime of a fuel element can therefore be carried out by considering the response of the simple rheological model (Fig.1). The actual stress distributions are obtained from the elastic solution multiplied by appropriate functions of dose, to be determined in the next chapter.

4. PARAMETRIC STUDY OF STRESSES IN A FUEL ELEMENT

In view of the analysis of thermal stresses and of stresses due to Wigner strains, the response of the rheological model (Fig.1) to an initial strain function $\varepsilon_0(\gamma)$ is considered.

$$\varepsilon_0(\gamma) = c_o + c_1(\gamma/\gamma_2) + c_2(\gamma/\gamma_2)^2 \qquad (11)$$

The first term is a step function and corresponds to the thermal dilatation field, the second and third terms are linear resp. parabolic ramp functions and they correspond to the Wigner strains (compare with (2)).

The Laplace transformation of (11) becomes:

$$\bar{\varepsilon}_0 = \frac{c_o}{s} + \frac{c_1}{\gamma_2\, s^2} + \frac{2c_2}{\gamma_2^2 s^3} \qquad (12)$$

4.1 Response to a Step Function

The Laplace transformation of the creep function (1) becomes:

$$\bar{J}(s) = \frac{1}{s} + \frac{a_1}{(1+\gamma_1 s)s} + \frac{1}{\gamma_2 s^2} \qquad (13)$$

The response of the rheological model (Fig. 1) on a step function c_o becomes:

$$\bar{\sigma} = - \frac{E\, c_o}{\bar{J}(s)s^2} \qquad (14)$$

After inversion one obtains:

$$\sigma(\gamma) = - E\, c_o\, f_o\, (\gamma)$$

$$f_o(\gamma) = \frac{\gamma_2}{\gamma_3-\gamma_4} \left\{ \left(1- \frac{\gamma_1}{\gamma_3}\right) e^{-\gamma/\gamma_3} + \left(\frac{\gamma_1}{\gamma_4} - 1\right) e^{-\gamma/\gamma_4} \right\} \qquad (15)$$

$$\frac{1}{\gamma_{3,4}} = \frac{1+a_1+ \frac{\gamma_1}{\gamma_2} \pm \sqrt{\left(1+a_1+ \frac{\gamma_1}{\gamma_2}\right)^2 - 4\, \frac{\gamma_1}{\gamma_2}}}{2\gamma_1}$$

The relaxation function f_o consists of two exponentials one with a smaller time constant and one with a greater one as compared to γ_1. In Fig.3 the function f_o has been plotted for various values of a_1 and γ_1/γ_2. The effect of primary creep is seen to act mainly in the beginning ($\gamma<\gamma_2$). For higher doses the effect of the primary creep is to relax the stress more slowly, although the difference is small. For the case where there is no primary creep the response on the step function becomes:

$$\sigma(\gamma) = - E\, c_o\, e^{-\gamma/\gamma_2} \qquad (16)$$

4.2 Response to a Linear Ramp Function

The response follows from the convolution theorem:

$$\sigma(\gamma) = - \frac{E\, c_1}{\gamma_2} \int_0^{\gamma} f_o(\gamma-\gamma')\, d\gamma'$$

$$= - E\, c_1\, f_1(\gamma) \qquad (17)$$

$$f_1(\gamma) = \frac{1}{\gamma_3-\gamma_4} \left\{ \left(1- \frac{\gamma_1}{\gamma_3}\right)\gamma_3\left(1-e^{-\gamma/\gamma_3}\right) + \left(\frac{\gamma_1}{\gamma_4} -1\right)\gamma_4\left(1-e^{-\gamma/\gamma_4}\right)\right\}$$

$$\lim_{\gamma\to\infty} f_1(\gamma) = 1$$

The function f_1 is given in Fig.4 for various values of the primary creep parameters. The effect of the primary creep is that the stationary value is reached more slowly. For the case of no primary creep the response becomes simply:

$$\sigma(\gamma) = -E c_1(1-e^{-\gamma/\gamma_2})$$
$$\sigma(\gamma)_{\gamma\to\infty} = -E c_1 \qquad (18)$$

It is noted that the stationary value does not depend on the primary creep parameters.

4.3 Response to a Parabolic Ramp Function.

The response follows from the convolution theorem:

$$\sigma(\gamma) = -\frac{2Ec_2}{\gamma_2^2}\int_0^{\gamma} f_1(\gamma-\gamma')d\gamma'$$
$$= -2 E c_2 f_2(\gamma)$$

$$f_2(\gamma) = \frac{1}{(\gamma_3-\gamma_4)\gamma_2}\{(1-\frac{\gamma_1}{\gamma_3})\gamma_3^2(\frac{\gamma}{\gamma_3}-(1-e^{-\gamma/\gamma_3})) + (\frac{\gamma_1}{\gamma_4}-1)\gamma_4^2 \cdot (\frac{\gamma}{\gamma_4}-(1-e^{-\gamma/\gamma_4}))\} \qquad (19)$$

$$f_2(\gamma)_{\gamma\to\infty} = (\frac{\gamma}{\gamma_2}-(1+a_1))$$

The function f_2 is given in Fig.5 for various values of the primary creep parameters. The effect of the primary creep is to delay the building up of the stresses. The asymptotic value does not depend on the primary creep time constant. For the case of no primary creep the response becomes simply:

$$\sigma(\gamma) = -2 E c_2\{\gamma/\gamma_2-(1-e^{-\gamma/\gamma_2})\}$$
$$\sigma(\gamma)_{\gamma\to\infty} = -2 E c_2(\gamma/\gamma_2-1) \qquad (20)$$

4.4 Combination of the three Responses

The parameter c_o is related to the variation of the thermal dilatation field over the structure. For given design and given power rating it is proportional to the ratio of thermal dilatation over thermal conductivity (α/λ). This gives rise to the definition of a figure of merit for graphite being the ratio of admissible stresses over generated thermal stresses $(\lambda\hat{\sigma}/\alpha E)$.

The stress distribution depends on the temperature distribution. In general it can be said that "hotter" places are subjected to -ve stress and "colder" places to +ve stress, the former being greater in absolute value due to the fact that "hot" spots are generally smaller than "colder" regions (This is due to the diffusion character of the temperature distribution and to the fact that conductivity decreases with temperature). Therefore as soon as the thermal stresses are relaxed (see Fig.3), relatively high tensile stresses are generated at the "hot" spots during shutdown periods.

The parameters c_1 and c_2 are related to the variation of the Wigner strain field over the structure. For given design and given power rating they are proportional to

$$\frac{1}{\lambda}\frac{d\,b_1}{dT} \quad \text{and} \quad \frac{1}{\lambda}\frac{d\,b_2}{dT},$$

b_1 and b_2 being the temperature dependent coefficients of the linear and parabolic ramp functions of the Wigner strain (2). The parameters b_1 and $\frac{d\,b_1}{dT}$ are negative and they cause therefore stresses in the same direction as those due to the thermal dilatation field at shutdown, i.e. tensile at "hot" spots. The parameters b_2 and $\frac{d\,b_2}{dT}$ are positive and they generate stresses in opposite direction.

As to the magnitude of the three mechanisms it is to be noted that the maximum dose of current H.T.G.R. fuel elements is in the order of 4.10^{21} nvt [7]. From Fig.2 it is seen that the turnover occurs at higher doses, and the contribution of the parabolic ramp function remains therefore negligible. (For other components with a higher integrated dose like H.T.G.R. reflector blocks or graphite fuel elements for breeder reactors, the parabolic contribution has to be taken into consideration). The stresses in an H.T.G.R. graphite fuel element depend therefore on two mechanisms, i.e. relaxed part of the thermal stresses at shutdown and stresses due to the linear part of the Wigner strains. The stress varies according to Fig.6 . The dose at which the steady state value is obtained depends on the primary and secondary creep parameters. However, for an integrated dose of 4.10^{21} nvt and a primary and secondary creep time constant of the order of 10^{20} nvt [7] it follows from Fig.3 and 4 that the maximum value will be obtained ($\gamma/\gamma_2 = 40$).

The contribution of the two mechanisms depends on α and $\frac{d\,b_1}{dT}\gamma_2$ respectively. Fig.7 gives the parameter b_1 as taken from various references. Although the scatter is rather big, it is possible as a first approach to correlate the data of each reference by a straight line, the slope of which gives the wanted value $\frac{d\,b_1}{dT}$. With a slope of -2.10^{-26} and a secondary creep time constant of the order of 10^{20} the contribution of the Wigner strain becomes proportional to 2.10^{-6} as compared to $\alpha = 5.10^{-6}$ for thermal stresses.

It is concluded that for H.T.G.R. fuel elements the contribution of the Wigner strains cannot be neglected, and, as a first approach, it can be taken into account by introducing a fictive coefficient of thermal dilatation:

$$\alpha^* = -\alpha + \frac{d\,b_1}{dT}\gamma_2 \tag{21}$$

A figure of merit for graphite can be defined, representing the ratio of admissible stresses over generated stresses ($\lambda\hat{\sigma}\,/\alpha^*E$). The stress distribution can be obtained from one single elastic solution introducing the fictive dilatation coefficients α^* (21).

5. Numerical Example

A typical H.T.G.R. tubular fuel element has been studied. The temperature distribution has been calculated by means of the two dimensional finite element code TAFE [2]. The results are plotted in Fig.8 by means of the code STRESS PLOT. The temperature distribution is introduced into the two dimensional thermo-elastic code ROTTEMP.

The stress distribution has been calculated for a fictive thermal dilatation coefficient (21) $\alpha^{*} = -7.10^{-6}$ and Young's modulus $E = 10^{3}$ kg/mm^{2}. Fig.9 shows the Calcomp plot of the equivalent stress according to the total stored elastic energy criterion defined by:

$$\sigma_{eq}^{2} = \frac{1}{E}\{\sigma\}^{T}[D]^{-1}\{\sigma\} \qquad (22)$$

This quantity is calculated at the centroids of the triangular finite elements and by an appropriate weighting procedure its values at the points are determined. The stress distribution is proportional to $\alpha^{*}E$, and the results for other material properties can readily be obtained.

REFERENCES

[1] DE ARRIAGA and RASHID
SAFE-CREEP, A computer program for the visco-elastic analysis of axi - symmetric and plane concrete structures. GA 8119 (1967)

[2] DONEA and GIULIANI
Comportement mécanique de structures complexes en présence de fluage, d'un champ de température et de variations de dimensions dues à l'irradiations. EURATOM Report, EUR 4629 (1971)

[3] GREENBAUM
Creep Analysis of Axisymmetric Bodies
Thesis, University of California (1966)

[4] CHANG, PUGH, MOORE
Visco-elastic Analysis of Graphite under Neutron Irradiations and Temperature Distribution. ORNL-TM-2407 (1969)

[5] CHANG, RASHID
Visco-elastic Response of Graphitic Materials in Irradiation Environment
GA-9820 (1969)

[6] KENNEDY
Creep of Graphite under Irradiation, pp. 198-203, GCRP Semiann.Progr.Rept. Sept.30, 1965, USAEC Report ORNL-3885, Oak Ridge National Laboratory; and Creep of Graphite under Irradiation, pp. 149 - 152, GCRP Semiann.Progr. Rept. March 31, 1966, USAEC Report ORNL-3951, Oak Ridge National Laboratory.

[7] EVERETT et al.
Graphite Behaviour in Relation to Fuel Element Design
D.P. Report 685 (1969)

[8] KASTEN et al.,
Graphite Behaviour and Its Effects on MSBR Performance,
Nuclear Engineering and Design, 9 (2): 157-195 (1969)

[9] LEE
Visco-elastic Stress Analysis, Chapter 53 in Handbook of Engineering Mechanics, edited by W. Flügge, McGraw-Hill, New York (1962)

[10] ZIENKIEWICZ, CHEUNG
The Finite Element Method in Structural and Continuum Mechanics
McGraw-Hill (1969)

$$\varepsilon = \frac{\sigma}{E}\left\{1 + a_1(1 - e^{-\gamma/\gamma_1}) + \gamma/\gamma_2\right\}$$

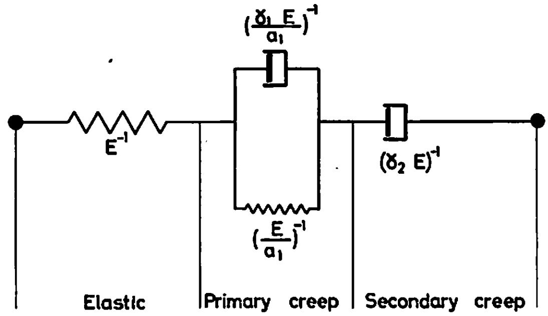

Fig. 1 Visco-elastic rheological model

$$\varepsilon = b_1\gamma + b_2\gamma^2$$

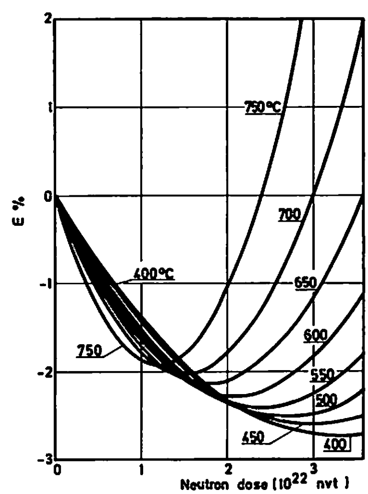

Fig.2 Neutron-Induced Dimensional Changes in Graphite at Various Temperatures [8]

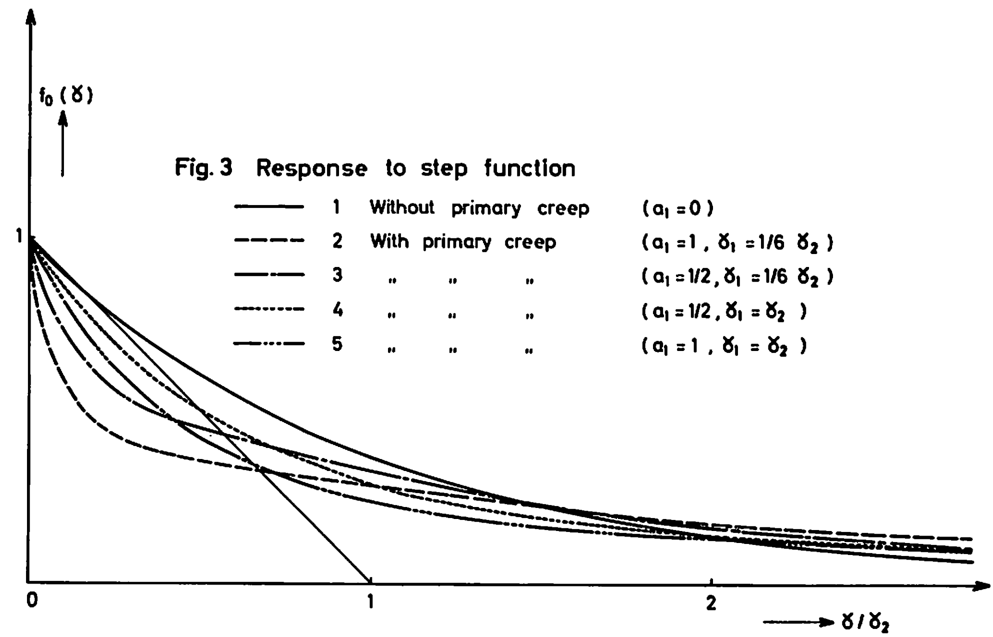

Fig. 3 Response to step function

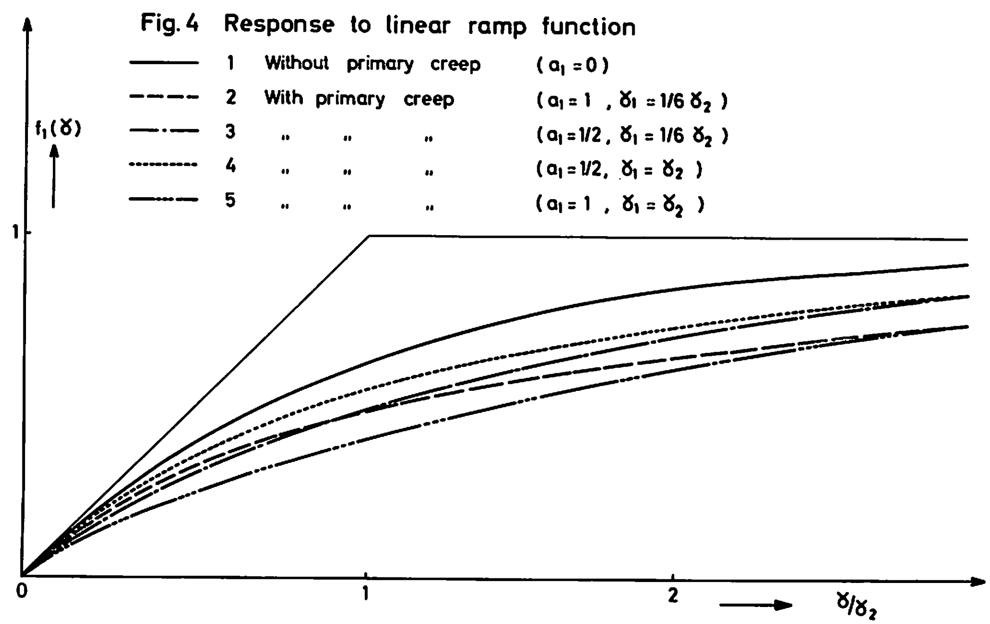

Fig. 4 Response to linear ramp function

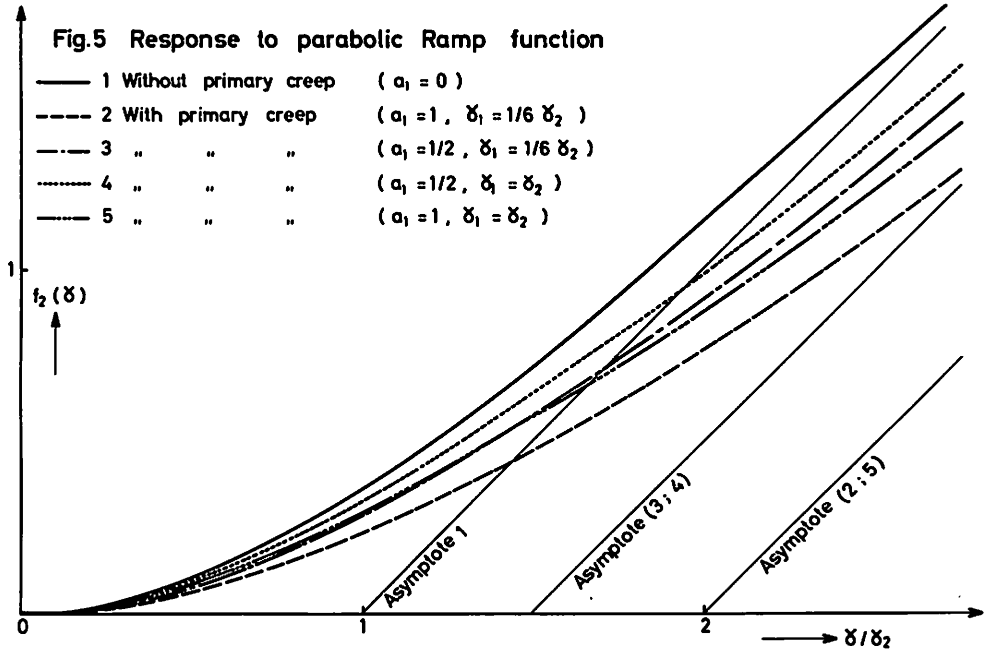

Fig.5 Response to parabolic Ramp function

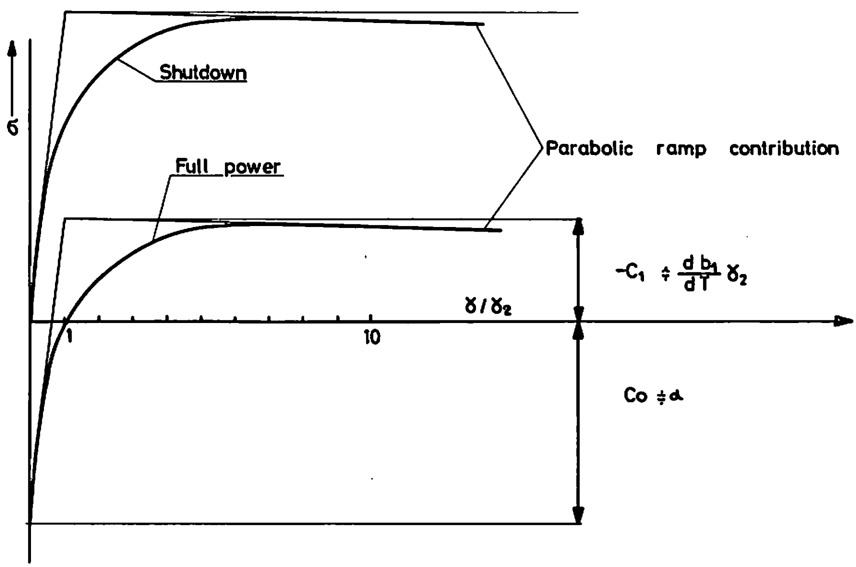

Fig.6 Stress evolution in graphite fuel element

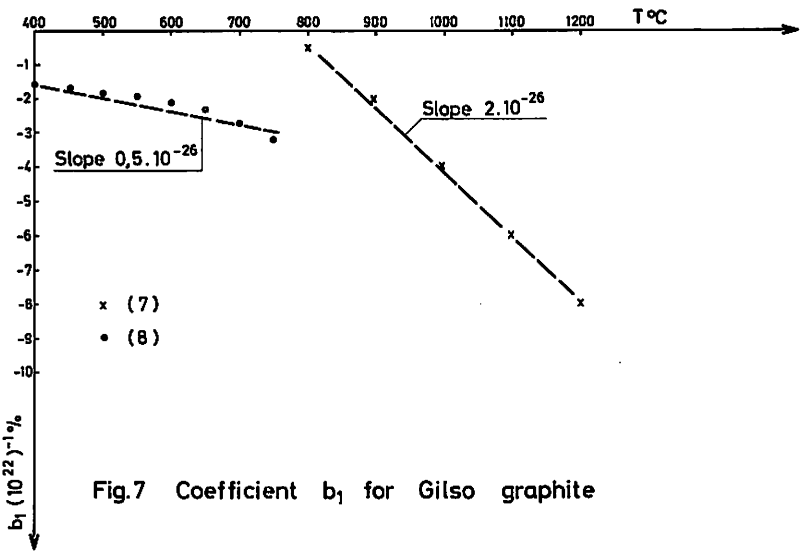

Fig.7 Coefficient b_1 for Gilso graphite

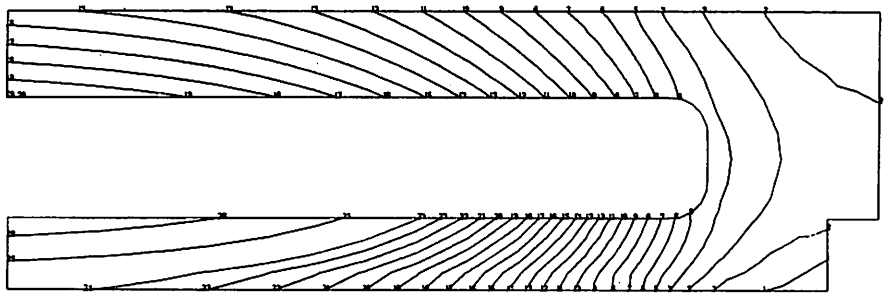

FIG. 8 Temperature distribution in H.T.G.R. tubular fuel element

level	1	770°C	10	860	19	950
	2	780	11	870	20	960
	3	790	12	880	21	970
	4	800	13	890	22	980
	5	810	14	900	23	990
	6	820	15	910	24	1000
	7	830	16	920	25	1025
	8	840	17	930	26	1050
	9	850	18	940		

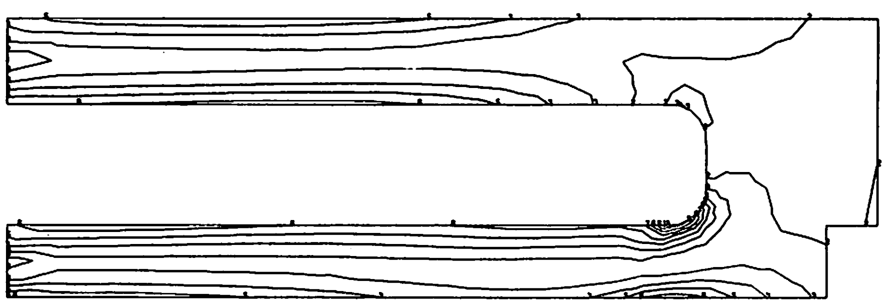

FIG. 9 Equivalent stress distribution in H.T.G.R. tubular fuel element

level	1	.004 Kg/mm^2	6	.326
	2	.068	7	.391
	3	.133	8	.455
	4	.197	9	.519
	5	.262	10	.583

$\dot{\varepsilon} . E = -7.10^{-3}$ Kg/mm^{2} °C

DISCUSSION

Q A. PHILLIPS, U. S. A.

Although I had no chance to study the paper, since it was not printed, I would like to ask the author whether in his opinion and experience the material used is really linear visco-elastic.

Q F. C. WEILER, U. S. A.

I would like to amplify the question asked by Prof. A. Phillips. I personally feel that if your material (graphite) is not truly linear elastic, then treating it as such, even for preliminary analyses, would produce meaningless answers for stresses and strains. Unfortunately, there are no short-cuts to obtaining the correct analysis.

A J. REYNEN, JRC Ispra, Italy

The questions on the applicability of the visco-elastic approach is a fundamental one. As outlined in the paper the method can be used in the early design stage to have quick answers on new designs. On the other hand it has been shown in the paper that the creep phenomenon is a fast one ($\gamma_2 \cong 10^{20}$ nvt = 20 days of full power of DRAGON reactor). This means that variations of γ_2 with time, which in practice are slow as compared to γ_2 can be accounted for by introducing the current value of γ_2.
As concerns the variation of γ_2 with space the effect on the thermal stresses is nil. (Thermal stresses "relax" full power and the design stress is therefore the "shutdown" thermal stress). Concerning the effect of the variation of γ_2 with space on the linear part of the Wigner strains, I have the feeling that the local values can be introduced in the elastic calculations. This is a feeling based on the principle of St. Venant, and I do not have a mathematical proof of it by hand, nor any numerical experience.